

ZENITH ANGLE AND DEPTH DEPENDENCE OF COSMIC RAY MUONS

H. E. Bergeson, G. W. Carlson, J. W. Keuffel, and J. L. Morrison
 Department of Physics, University of Utah
 Salt Lake City, Utah 84112

The Utah experiment on angular distribution of TeV cosmic ray muons has been repeated with improvements in the detector and in the analysis. The results agree with expectation based on pion and kaon parentage of the muons. A muon intensity vs. depth curve of high statistical accuracy is presented.

1. Introduction. The zenith angle dependence of cosmic ray muons in the TeV range has been the center of lively interest at the last 3 conferences in this series. The subject is of central importance, since an anomalous, isotropic muon component which did not exhibit the $\sec \theta$ enhancement expected for muons from pion and kaon decay would signal the existence of a strongly-produced massive parent particle with a strong branching ratio for decay into muons.

Previous studies of the effect from this laboratory (Bergeson et al. 1971a) had indicated the existence of such an anomalous muon component. A number of experiments sought to confirm or deny the effect, but it is probably fair to say that a firm consensus had not been reached at the time of the Hobart Conference (Bergeson et al. 1971b).

This paper reports a complete repetition of the Utah experiment based on 2.2×10^5 muons obtained in 1971-72 with improved Cherenkov detectors and a new analysis. The new results are in satisfactory agreement with the conventional picture of pions and kaons as the sole parents of the muons.

Once this picture is accepted, the angular dependence of the Utah data is known and the way is open to construct a vertical intensity vs. depth curve of good statistical accuracy. This permits one to investigate the primary spectrum and models of hadronic interactions.

2. Modifications to the Cherenkov Counters. For the present runs, the Cherenkov counters were rebuilt with new light collectors as described by Cassidy et al. (1973). With the light collection improved by about a factor 5, the overall efficiency of the new detector lay between 90% and 95% at all angles and did not deteriorate appreciably with time. It was still necessary to calibrate the efficiencies continuously during the run as before, using events where at least 3 Cherenkov detectors were struck by muons; but more accurate results could be obtained than with the old Cherenkov system, where the overall efficiency had steadily deteriorated with time until at the end it ranged from 40% to 70%. In spite of this difference in efficiencies, the muon intensities from the 1969 run were only about 5% lower than those from the '71-'72 runs.

Apart from the Cherenkov modification the apparatus was essentially the same as in our previous work.

3. Analysis of the Data. The muon intensity as a function of slant depth and zenith angle θ is desired. The magnetic tapes are scanned for single muon events, which constitute the bulk of the data, using the automatic pattern recognition program GSORT. If an event contains two or more muons ($\sim 5\%$ for our large detector) each muon is treated individually. Muons are assigned to $2.5^\circ \times 5^\circ$ zenith-azimuth bins, and the intensity for each bin computed from the number of muons divided by the appropriate aperture \times solid angle factor, Cherenkov and spark counter efficiencies, and running time. A value of h is assigned to each bin using topographical maps and a density of 2.55 gm/cm^2 measured by Cassidy et al. (1972).

Data in bins within $h/2$ of a given central slant depth h are combined after a centering correction taken in the first instance from a conventional π - and K -derived expectation for $I(h, \theta)$ and then iterated using the $I(h, \theta)$ functions which fit our own data. The iteration is simple and reliable since the depth dependence is practically the same whether or not an isotropic component is present.

The analysis proceeds as in Bergeson et al. (1971a) by writing

$$I(h, \theta) = I_{\pi K}(h) G(h, \theta) + I_X(h) \quad (1)$$

The calculated function $G(h, \theta)$ exhibits the expected angular enhancement and differs from $\sec \theta$ by only a few percent over our range of parameters. We then fit our data to the function (1) and ask whether an isotropic component I_X is required. In Figs. 1 and 2 are shown muon intensities for central depths of 3200 and 4800 hg/cm^2 ($1 \text{ hg/cm}^2 = 100 \text{ g/cm}^2$ of standard rock), plotted against G , rather than $\sec \theta$, to make fits given by (1) (which are also shown) straight lines. The ratio of charged kaon and pion fluxes at production by the nucleon flux was taken to be 0.09 as predicted by scaling of accelerator data (Morrison and Elbert 1973).

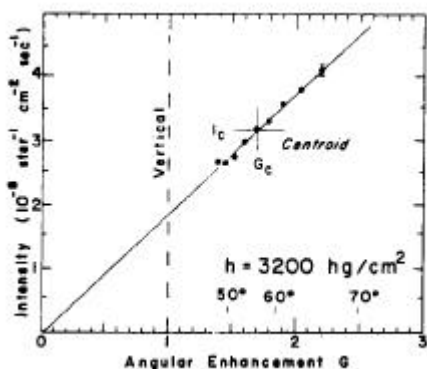


Fig. 1. Zenith angle distribution of muon intensities at 3200 hg/cm^2 ($G = \sec \theta$; see text).

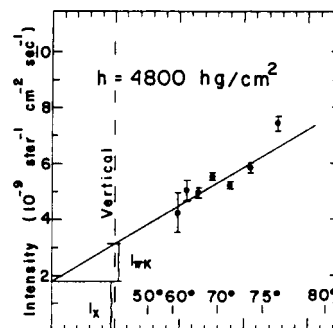


Fig. 2 Same as Fig. 1 but at 4800 hg/cm^2 . The intercept at $G = 0$ gives a measure of the isotropic component indicated by the data shown.

The results of the fit at a given depth can be conveniently separated into a centroid and a slope so that the errors are decoupled. The slopes alone suffice to give the ratio $f_X = I_X/I_V$, where I_V is the vertical intensity; a non-zero f_X is evidence for an isotropic muon component. This method of analysis depends on the Utah data alone.

A second type of analysis introduces data from a world survey of vertical muon intensities which yield a point at $G = 1$ for each such graph as shown in Figs. 1 and 2. Combining these with the centroids of our curves, one arrives at an independent set of values for f_X . This second method is far less sensitive to the Utah intensities but depends of course on the adopted vertical intensity curve and requires a precise knowledge of the density of Utah rock relative to the world average.

4. Results Using Utah Data Only. The results of the first method of analysis are shown in Fig. 3. Values of f_X were obtained from 6 plots of the type shown in Figs. 1 and 2. In assigning error flags, the statistical errors of each fit have been multiplied (for $S > 1$) by a factor S so chosen that, if each individual intensity error flag in the plots of the type of Figs. 1 and 2 is multiplied by S , the resulting χ^2 for the fit has the value expected for the number of degrees of freedom involved. The values of S are indicated in Fig. 3. This procedure takes into account errors due to random fluctuations in the rock density, for example, but systematic trends may of course still be present. (Rock density fluctuations are discussed below.) It is noteworthy that the two points for which the deviation of f_X from zero is at all significant are the ones having the largest X -values and the poorest fit. On the other hand, the point at 3200 hg/cm^2 has $f_X = 0.1 \pm 0.07$ and has a small S -value. The smoothness of the 3200 hg/cm^2 plot (Fig. 1) is understandable, since at this depth each point is the consolidation of many different bins averaging over many different samples of rock. Thus at this depth the first method (Utah data alone) implies $f_X < 0.1$, and at greater depths the data are all consistent with no isotropic component.

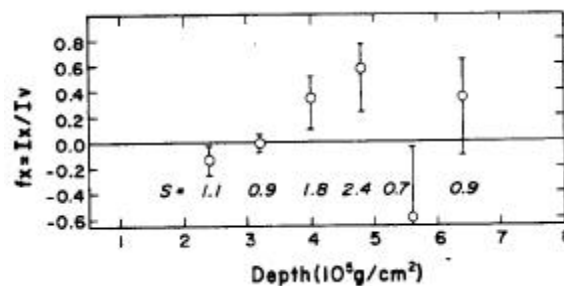


Fig. 3. Ratio of isotropic component to vertical muon intensity as inferred from Utah data alone.

5. Results with World-Survey Vertical Intensities Included. In order to evaluate the $f_X(h)$ using the second method mentioned above, a world-survey vertical muon intensity-depth curve was prepared. Points from a world survey by Groom (private communication) were fitted with functions recently calculated by Carlson (1973). Muon surface spectra were folded into rigorous muon survival probabilities also calculated by Carlson, and the fit determined by variation of the parameters of the surface spectra. One such muon spectrum was derived from a power-law pion and kaon production spectrum having a constant spectral index γ . It gave the two-parameter fit shown in curve A in Fig. 4, with $\gamma = 2.68 \pm 0.02$ and $\chi^2 = 37$ for 20 degrees of freedom. Curve B was a three-parameter-fit with a slowly-varying index $\gamma = \gamma_0 + a \ln E$, with $\gamma_0 = 2.63 \pm 0.02$ and $a = 0.57 \pm 0.015$ with E_i in TeV. It gave a better fit, with $\chi^2 = 19$ for 19 degrees of freedom. We¹ adopted

curve B as our standard; representative values of the intensity are 6.9×10^{-8} , 2.29×10^{-9} , and $1.3 \times 10^{-10} \text{ cm}^{-2} \text{ s}^{-1} \text{ sr}^{-1}$ at depths of 2.4×10^5 , 4.8×10^5 , and $7.2 \times 10^5 \text{ g cm}$ of standard rock. The experimental points, and curve A, are shown in Fig. 4 relative to this standard.

Vertical intensities from curve B may now be combined with the centroids of our I-vs.-G curves to yield values of f_x according to the second method outlined above. The results are shown in Fig. 5 as open circles. We also show the values of f_x which are obtained if one chooses for the density of Utah rock $\rho = 2.59$, the density at the 1 s.d. upper limit given by Cassidy et al. (1971), rather than at the central value 2.55. Thus one does not need to invoke unreasonable densities to bring the values of f_x down to zero, and we conclude by this method also that no isotropic muon component is required.

6. Discussion. The important sources of error are (a) the Cherenkov counterefficiencies, (b) the rock density, and (c) the adopted vertical intensity curve. The efficiencies have already been discussed in Sec. 2 and a further check is discussed in connection with Fig. 6; errors from this source are now believed to be small compared to those from (b). The best measurement of the density is that of Cassidy et al. (1971), who measured the vertical muon intensity at ten locations along the access tunnel to the main detector, and by comparison with the world-survey curve deduced $\rho = 2.55 \pm 0.04$. Direct measurements of the density are limited in the number of points of access where samples can be taken, but an average of 2.61 was adopted by Keuffel et al. (1969). A measure of the fluctuations in mean density encountered by muons arriving at the detector from various directions is provided by a so-called Larson plot as shown in Fig. 6. The number of muons in each of $96 \text{ } 5^\circ \times 20^\circ$ zenith-azimuth bins is compared with the expectation based on a conventional pion and kaon derived underground muon intensity function. If each $5^\circ \times 20^\circ$ bin is assigned a random density error of 1.3%

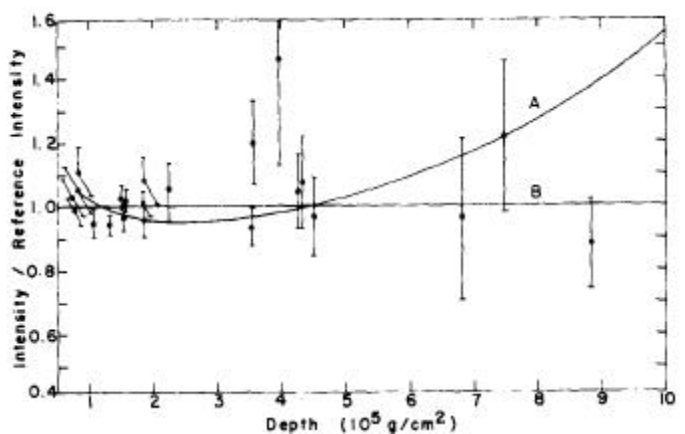


Fig. 4. Fits to a world survey of vertical muon intensities. Error flags have been enlarged to allow for 1% density errors. Curve B, the reference intensity, has a gradually steepening meson production spectrum index while for curve A the index is constant. (See text.)

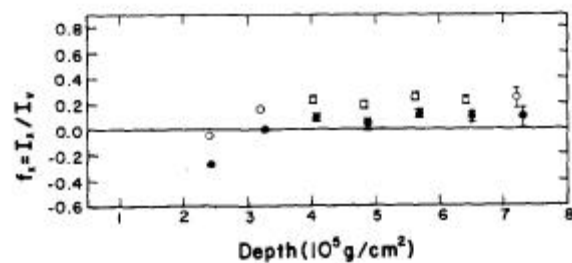


Fig. 5. Ratio of isotropic component to vertical muon intensity as inferred from Utah centroid intensities and world-survey vertical intensities. The error band for the fit to vertical intensities gives added errors of 0.05 - 0.08 in f_x .

the fit becomes quite good ($\chi^2 = 96$ for 106 degrees of freedom.) Density fluctuations of this magnitude are consistent with the Cassidy results (1.6%).

The Larson plot also checks the topographical studies, the automatic scanning program, and the overall efficiency. The efficiency calibrations show a small dependence on the angle to the normal of the Cherenkov detectors; this angle changes drastically even for constant zenith angle as one looks at different azimuths, so that the azimuthal constancy of the Larson plot tests the angular dependence of the efficiency.

The functional form of our adopted vertical intensity curve is derived from a realistic surface muon spectrum--a very important consideration since the vertical intensity data are sparse over rather large intervals of depth. The improvement brought by this vertical intensity fit was the most important single improvement of the present experiment over our previous work, for roughly speaking, the spurious contributions to f_X as found by method 2 in our early work were: density, 0.1; efficiency, 0.05-0.1; and vertical intensity curve, 0.3. Of course, for method, 1 the efficiencies were the critical factor, but we had placed great stress on method 2. Unfortunately, the two methods agreed fairly well on a positive f_X 0.5 but erred for different reasons.

Once the muon angular dependence is assumed to follow the conventional model, our data may be combined and corrected to the vertical by the appropriate G factor. Such a vertical intensity curve is shown in Fig. 7. We have adopted

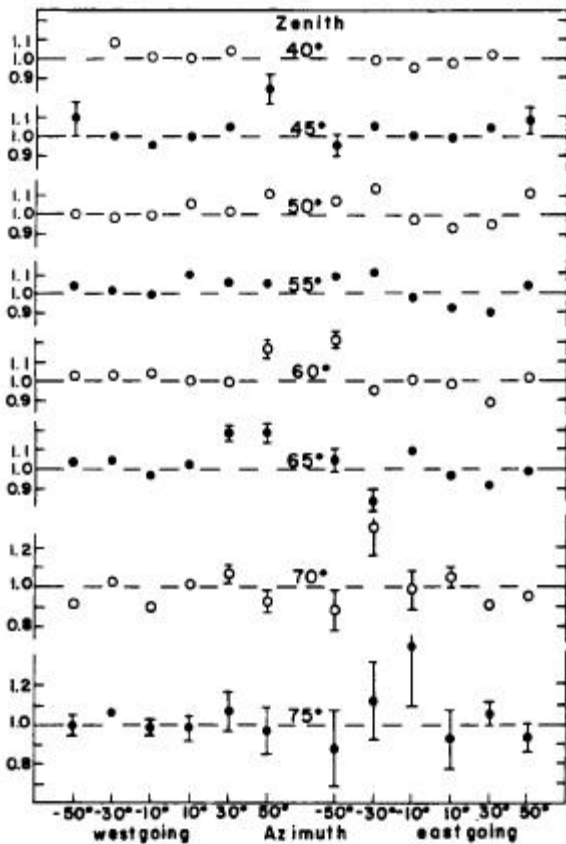


Fig. 6. Ratios of measured intensities to conventional model expectations. (Larson plot)

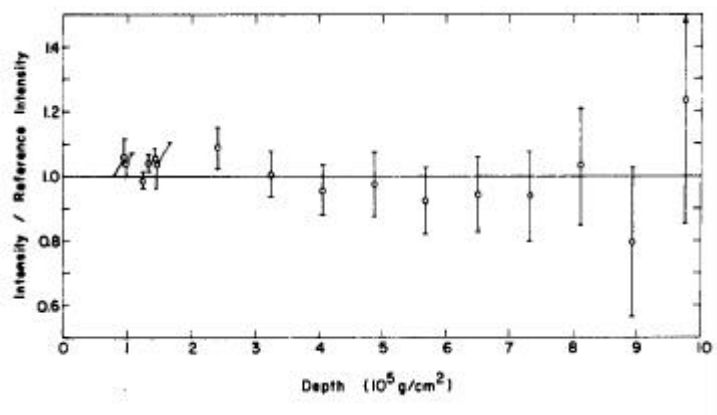


Fig. 7. Vertical intensities inferred from Utah data.

the density 2.59 called for to bring the angular dependence into consonance with the adopted world-survey vertical curve, but have increased the error flags to allow for a 1% density fluctuation. Fitting these points with a function derived from $\gamma = \gamma_0 + a nE$ we obtain $\gamma_0 = 2.64 \pm .03$ and $a = .073 \pm 0.021$, in excellent agreement with the previous fit to the world points. Note that zenith angle errors due to scattering, topographical, and instrumental effects will, if anything, tend to increase the steepening effect we observe (larger a).

The steepening of the muon spectrum could be explained by a failure of scaling in hadronic collisions, an increase in muon energy loss in the rock, or a steepening of the primary spectrum. The observed steepening is consistent with a cut-off of the primary nucleon spectrum near 200 TeV (Elbert et al. 1973).

The question of the kaon to pion ratio for the parents of the muons cannot be answered with much precision from this experiment. A fit to the data at $3.2 \times 10^5 \text{ g/cm}^2$ (Fig. 1) where the angular dependence is best determined, gave a value of f_X (regarded here as a measure of the fit with no isotropic component) of $-0.07 \pm .09$ when the angular enhancements were based on a ratio of charged kaon to charged pion flux at production of 0.43. With the scaling-derived value of 0.09 for the ratio, f_X was close to zero, indicating a preference for the lower K / π ratio.

The limit $f_X < 0.1$ implies a limit on the cross section for the production of a massive particle which undergoes a two-body high-Q decay into $\bar{\nu} + ?$ is $\sim 0.1 \text{ mb/nucleon}$, depending on the model adopted.

Acknowledgement. This work was supported by the National Science Foundation (USA).

References.

- Bergeson, H. E. et al. 1971a, Phys. Rev. Letters 27, 1960. _____ 1971b, Proc. 12th Int. Conf. on Cosmic Rays (Hobart, Tasmania).
 Carlson, G. W. 1973, Thesis, University of Utah (unpublished).
 Cassidy, G. L. et al. 1971, Phys. Rev. Letters 27, 164.
 Keuffel, J. W. et al. 1969, Acta Physica Acad. Sci. Hungaricae 29, Suppl. 4, 183.
 Morrison, J. L. and Elbert, J. W. 1973. Paper in OG section of these proceedings.

Filename: icrc733-1722
Directory: C:\WINDOWS\Desktop\Amy's Papers
Template: C:\Program Files\Microsoft Office\Templates\Normal.dot
Title:
Subject:
Author:
Keywords:
Comments:
Creation Date: 07/22/01 5:31 PM
Change Number: 5
Last Saved On: 08/23/01 9:33 AM
Last Saved By: user
Total Editing Time: 282 Minutes
Last Printed On: 10/08/01 11:29 AM
As of Last Complete Printing
Number of Pages: 7
Number of Words: 2,134 (approx.)
Number of Characters: 12,164 (approx.)